# The Influence of linear Heating on Free Convection in a Cylindrical Enclosure

AKRAM MAZGAR[1,2], BEN NEJMA FAYCAL[2]
[1]Ionized and Reactive Media Studies Laboratory,
Preparatory Institute for Engineering Studies of Monastir,
University of Monastir,
Ibn Eljazar Street 5019 Monastir,
TUNISIA

[2]Higher Institute of Applied Sciences and Technology,
University of Sousse,
Taher Ben Achour Street 4003 Sousse,
TUNISIA

*Abstract:* - The current study aims to numerically investigate free convection airflow within a horizontal cylinder with a linearly heated side wall. The computation of heat transfer and fluid flow structure has been carried out using the finite element software COMSOL Multiphysics. The influence of the heat source position on fluid flow and heat transfer is inspected. Special attention is paid to the effect of Rayleigh number and the heater position on energy efficiency within the cavity. The results indicate that the best heat transfer performance is achieved for low Rayleigh numbers and when the active wall is centered in the vicinity of 90°.

*Key-Words:* - Free convection, linear heating, cylindrical enclosure, energy efficiency, COMSOL Multiphysics, heat transfer.

Received: May 16, 2023. Revised: October 17, 2023. Accepted: December 8, 2023. Published: December 31, 2023.

## 1 Introduction

The rise in popularity of heat transfer induced by free convection has been notable in recent times, primarily because of its autonomy from external energy sources, [1], [2], [3], [4]. Commonly referred to as the buoyancy effect, natural convection is employed to improve heat transfer in diverse engineering fields. This includes applications in building insulation, food storage processes, cooling of metals and electronic components, and various other domains.

The free convection challenge within an enclosure encompasses the boundary layer flow near the boundaries and the internal flow region beyond the boundary layer. Consequently, the heat transfer from the cavity wall is shaped by both the specified boundary conditions and the thermophysical characteristics of the working fluid within the cavity. In many previous studies, a common methodology involves uniformly heating one wall of the cavity while uniformly cooling the opposite wall. This scenario, known as the conventional natural convection problem, typically employs air as the working fluid. The interplay of temperature distribution and fluid flow significantly affects heat transfer induced by free convection in enclosures. Consequently, the defined boundary conditions at the control volume walls have a substantial impact on the heat transfer from the cavity. In the majority of instances, the cavity experiences uniform heating or cooling from the wall, [5], [6], [7], [8], [9]. Employing such uniform heating can produce reasonably accurate results when calculating the thermal performance of numerous configurations of interest. However, practical scenarios often arise where the impact of non-uniform wall heating must be considered, [10]. This type of process exists in several industrial applications, such as addressing specific heating needs, minimizing undesirable temperature variations, and using heat transfer at different temperatures in different areas of the installation, etc. An example of specific burners can be cited, used for heat treatment applications or for non-uniform heating zones to meet particular requirements. This phenomenon frequently influences thermal performance in various industrial applications. This is why many researchers have directed their attention toward understanding the influence of non-uniform heating on heat transfer

phenomena and fluid flow properties. [11], examined the impact of both uniform and non-uniform heating on free convection within a trapezoidal enclosure. Their findings indicated that introducing non-uniform heating to the bottom wall leads to an enhancement of the rate of heat transfer at the midpoint of the bottom wall when compared to the scenario with uniform heating, a trend observed across all Rayleigh numbers. However, it's noteworthy that the mean Nusselt number consistently suggests a generally reduced heat transfer rate for the case with non-uniform heating. In their study [12], the authors utilized heatline visualization techniques to examine the heat and fluid flow in an inclined cavity subject to non-uniform heating and filled with CuO nanofluids. Their results suggested that non-uniform hot wall temperatures induce the formation of small closed cells at the top of the hot wall, particularly for uninclined cavities. In a distinct investigation [13], delved into the influence of both the height and location of an obstacle on free convection within a square cavity. In this setup, the cavity experienced linear heating from the side walls, uniform cooling from the bottom wall, and insulation on the top wall. The study uncovered that when the obstacle is located on the lower wall, this not only induces the formation of a strong circulation cell but also a weaker one within the cavity. Moreover, the obstacle, characterized by high thermal conductivity, led to a reduction in heat exchanges with the lower wall and an increase in heat exchanges with the side walls. In their study [14], inspected heat transfer induced by free convection in a square differentially-heated cavity, where variations in the temperature of the left wall either increased or decreased linearly along the wall, along with similar variations in the right wall temperature. Particularly noteworthy is the outcome observed when the right wall's temperature rises linearly and the left wall's temperature diminishes linearly, resulting in the formation of two flow cells within the enclosure, one at the bottom and the other at the top. Additionally, [15], demonstrated the impact of the linear position of heating on entropy creation due to free convection in a square cavity. Their findings highlighted that the position of the linear heating center significantly influences both heat transfer and entropy creation resulting from natural convection. The study indicates that when the linear heating center is elevated, the fluid flow shifts to the right, accompanied by a concurrent reduction in its intensity. However, there is a substantial increase in heat transfer under these conditions. In [16], the authors examined horizontal convection in a rectangular cavity with linear temperature distribution. Their findings revealed that the examination of mean flows indicated a decrease in the kinetic and thermal boundary layer thickness, as well as the average temperature in the bulk region, as the Rayleigh number increased. [17], conducted a numerical investigation into the process of non-uniform wall heating of a square cavity and the resulting free convection. The study concluded that the optimal heat transfer rate is achieved when the heating occurs near the top wall of the heated boundary. [18], numerically investigated free convection in a porous cube under non-uniform heating. They mentioned that the presence of the porous layer causes the enhancement of heat exchanges. [19], studied the influence of non-uniform heating on velocity and temperature distributions of free convection within a vertical duct of a prismatic modular reactor core. They concluded the temperature differences between the wall and the fluid, along with axial variations in velocity distributions reveal flow instabilities at the top wall of the channel. [20], conducted experimental research on the heat exchange performance of high-temperature heat pipe exposed to axial non-uniform heat flux. Their findings indicated that the most promising performance of heat transfer and temperature uniformity are detected if the heating power is adjusted to 1133.7 W. Recently, [21], reported the 2D flow micropolar nanofluid in mixed convection with unsteady circumstances and non-uniform heat source/sink. They found that the variables related to unsteadiness and magnetism tend to increase the motion of the fluid.

In summary, various boundary conditions such as uniform, non-uniform (sinusoidal), or linear heating, have been specified for control volume walls in the literature. However, the effects of linear heating on free convection have not been adequately studied, even less for cylindrical geometry. The main goal of the current research is to explore the influence of the center of the heater location on free convection in a cylindrical enclosure and determine the optimal level of energy efficiency.

## 2 Problem Description

The present article model refers to a cylindrical wall containing air (Pr = 0.71) and exposed to linear heating. COMSOL Multiphysics software is applied to model the comportment of flow field and heat exchange processes.

In this study, the defined dimensionless parameters are given as follows:

$$X = \frac{x}{R}$$

$$Y = \frac{y}{R}$$

$$r = \sqrt{X^2 + Y^2}$$

$$U = \frac{uR}{\alpha}$$

$$V = \frac{vR}{\alpha}$$

$$\Theta = \frac{T - T_c}{T_h - T_c}$$

$$\Pi = \frac{PR^2}{\rho\alpha^2}$$

$$Pr = \frac{\nu}{\alpha}$$

$$Ra = \frac{g\beta}{\nu\alpha} R^3 \Delta T$$

A linearly heated boundary condition is externally imposed along the wall:
$\theta(\phi) = 1 - \left|\frac{\phi - \phi_0}{\pi}\right|$ where $\phi \in ]-\pi + \phi_0, \pi + \phi_0[$

Figure 1 shows the linear temperature distributions on the walls for $\phi_0 = 0°$.The red line indicates the boundary between the region where the imposed dimensionless temperature is higher or lower than 0.5. Note that heat exchange process occurs from the fluid to the wall even in areas where $\Theta > 0.5$ and conversely, the wall heats the fluid in certain areas even for $\Theta < 0.5$.

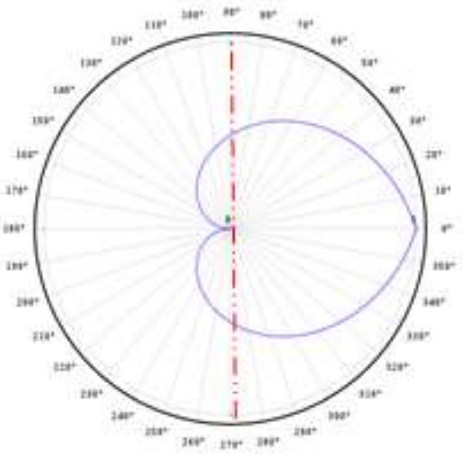

Fig. 1: Linear temperature distribution; $\phi_0 = 0°$

After the variable substitution, the governing dimensionless equations are expressed as the following:

$$\frac{\partial U}{\partial X} + \frac{\partial V}{\partial Y} = 0 \quad (1)$$

$$U\frac{\partial U}{\partial X} + V\frac{\partial U}{\partial Y} = -\frac{\partial \Pi}{\partial X} + Pr\left(\frac{\partial^2 U}{\partial X^2} + \frac{\partial^2 U}{\partial Y^2}\right) \quad (2)$$

$$U\frac{\partial V}{\partial X} + V\frac{\partial V}{\partial Y} = -\frac{\partial \Pi}{\partial Y} + Pr\left(\frac{\partial^2 V}{\partial X^2} + \frac{\partial^2 V}{\partial Y^2}\right) + PrRa\Theta \quad (3)$$

$$U\frac{\partial \Theta}{\partial X} + V\frac{\partial \Theta}{\partial Y} = \frac{\partial^2 \Theta}{\partial X^2} + \frac{\partial^2 \Theta}{\partial Y^2} \quad (4)$$

Certainly, taking into account that the local Nusselt number at the heated wall serves as a crucial metric for characterizing heat exchange between the gas and the walls. It is formulated in accordance with equation (5).

$$Nu_l(\Phi) = -2\left.\frac{\partial \Theta}{\partial r}\right|_{r=1,\Phi} \quad (5)$$

Furthermore, the calculation of mean Nusselt numbers for the heated wall is conducted to obtain a comprehensive understanding of heat transfer throughout the enclosure. This provides an overarching perspective on the overall heat transfer characteristics within the system. It is expressed as follows:

$$Nu = \frac{1}{\Phi_2 - \Phi_1}\int_{\Phi_1 \max(0,Nu_l(\Phi))>0}^{\Phi_2 \max(0,Nu_l(\Phi))>0} \max\left(0, Nu_l(\Phi)\right) d\Phi \quad (6)$$

or quite simply:

$$Nu = \frac{1}{4\pi}\int_0^{2\pi} |Nu_l(\Phi)| d\Phi \quad (7)$$

In addition, the efficiency of energy utilization in the current process is defined to provide insight into the minimum energy required to sustain a constant mean temperature. This measurement acts as a valuable indicator of the heating effectiveness of the system in maintaining thermal stability while minimizing energy. The corresponding expression is given in equation (8).

$$\varepsilon = \frac{\Theta_a}{2Nu} \quad (8)$$

The computation of the mean dimensionless temperature and velocity, as outlined in Eq. (9), is undertaken to enhance the understanding of fluid flow and heat exchange processes. These averages are expressed as follows.

$$\begin{cases} \Theta_a = \frac{1}{\pi}\int_0^{2\pi}\int_0^1 \Theta r dr d\phi \\ \mathrm{U}_a = \frac{1}{\pi}\int_0^{2\pi}\int_0^1 \sqrt{U^2 + V^2} r dr d\phi \end{cases} \quad (9)$$

# 3 Numerical Procedure

Please note that solving the partial differential equations in the COMSOL modeling environment is accomplished by employing an implicit scheme, utilizing the damping Newton technique within an adaptive automatic triangular grid. Notably, a mesh refinement strategy is implemented in proximity to boundaries, as illustrated in Figure 2. The mesh configuration comprises 21,014 domain elements and 472 boundary elements.

As evident from Table 1, the use of an automatic normal grid appears to be sufficient, but in practice and for more precision, we opted for an automatic extremely coarse grid and the error does not exceed $8.10^{-3}$ %.

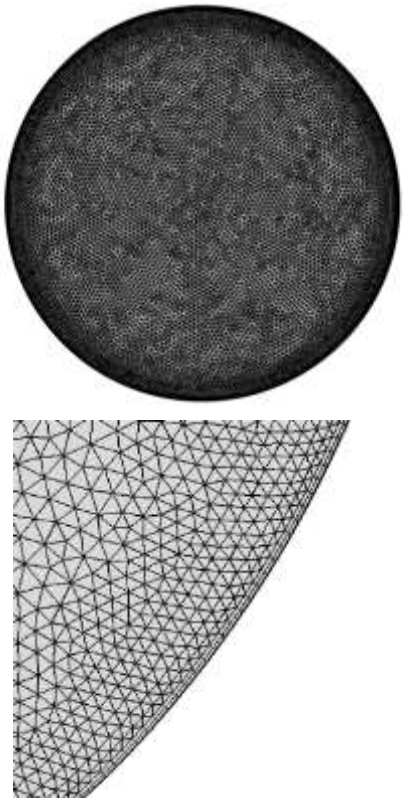

Fig. 2: COMSOL grid resolution

Table 1. Grid effect ($\phi_0$=0)

| Solver automatic grid | Nu ($Ra=10^4$) | Nu ($Ra=10^5$) |
|---|---|---|
| *Extremely coarse* | *2.0167* | *3.7982* |
| *Extra coarse* | *2.0166* | *3.7985* |
| *Coarse* | *2.0163* | *3.8006* |
| *Fine* | *2.0192* | *3.7990* |
| *Normal* | *2.0177* | *3.7892* |

# 4 Problem Solution

The calculations were conducted for a Prandtl number (Pr) of 0.71 within the range of $10^4 \leq Ra \leq 10^6$. The obtained results are presented in Figure 3, Figure 4, Figure 5, Figure 6, Figure 7, Figure 8, Figure 9 and Figure 10, aiming to provide a comprehensive analysis of the impact of linear heating devices on fluid flow and heat exchange processes. For instance, Figure 3, Figure 4, Figure 5, Figure 6 and Figure 7 depict the local fields of Nusselt number, velocity, and temperature for various locations of the heat source center at Ra = $10^5$. Upon initial observation, the Nusselt numbers exhibit similar profiles regardless of the heater's location but deviate from the expected flattened to elongated profile. Notably, the specific profile of the Nusselt number is of interest when the heater is centered at 90°, prompting consideration of thermal conduction between the heated and cooled walls. Returning to Figure 3, which illustrates the local distributions when the heater is centered at -90°, it should be noted that reference must be made to the fact that the flow velocity exhibits an asymmetric profile despite the use of symmetry conditions. The corresponding fields show a single rotating and elongated convection cell spanning the entire domain. Also, it should be mentioned that the temperature profile given in Figure 3c displays a zone of average temperature in the middle of the cavity.

Figure 4 depicts the local distributions when the center of the heater is located at -45°. At first blush, we can signal that the Nusselt number profile is more elongated, displaying a peak heat exchange located where the temperature is extreme. The fluid flow is visibly accelerated resulting in a multicellular flow with a practically symmetrical profile, following circular streamlines and displaying higher velocities. The center of the cavity seems to be in slow motion, featuring multiple cells. What is noteworthy in Figure 5 when the heater is centered at 0°, is that the Nusselt number distributions are more developed and the flow patterns display an asymmetric profile.

The local distributions of Figure 6 mention that the Nusselt number profiles are less elongated and the fluid flow exhibits a central zone containing a single cell at the center of the cavity with two discrete foci located at the extremities of the cell. Additionally, it is essential to indicate the formation of elliptical streamlines with the existence of a bicellular flow in the middle of the cavity. It is noteworthy also that the central multicellular zone tends toward an elliptical shape as the center of the source approaches 90°.

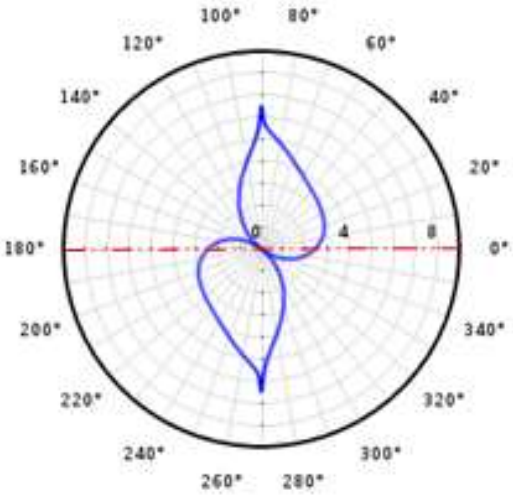


(a)

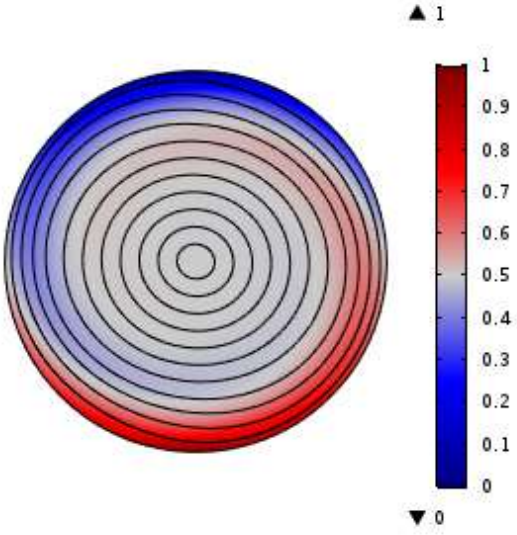


(b)

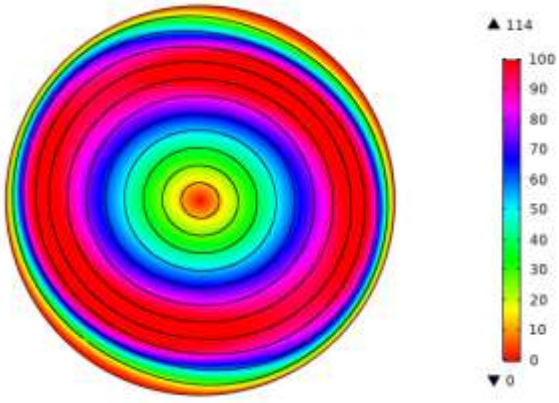


(c)

Fig. 3: Local distributions; Ra = $10^5$, $\phi_0 = -90°$
*(a) Nusselt number; (b) dimensionless velocity; (c) dimensionless temperature*

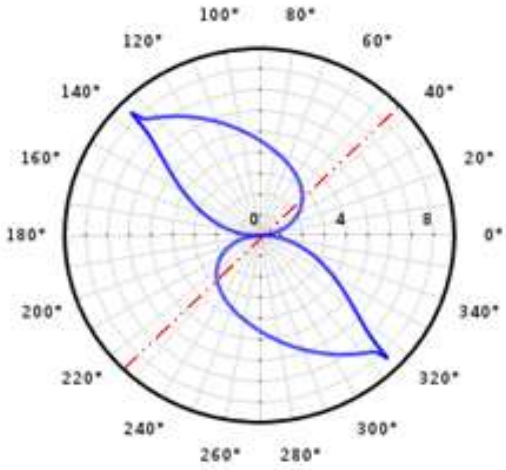


(a)

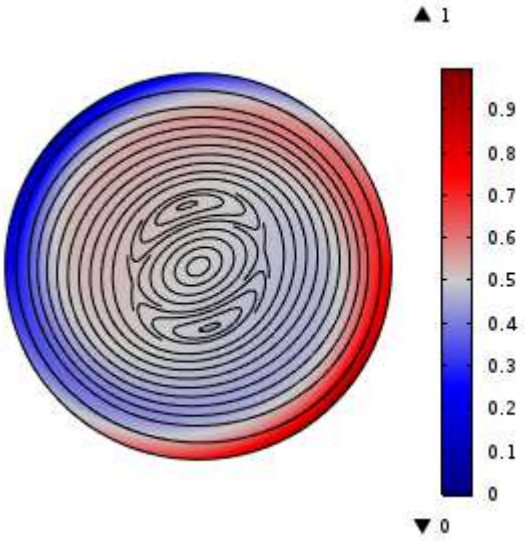


(b)

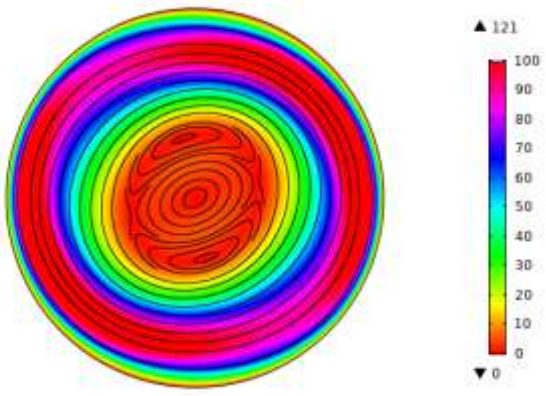


(c)

Fig. 4: Local distributions; Ra = 105, $\phi_0 = -45°$
*(a) Nusselt number; (b) dimensionless velocity; (c) dimensionless temperature*

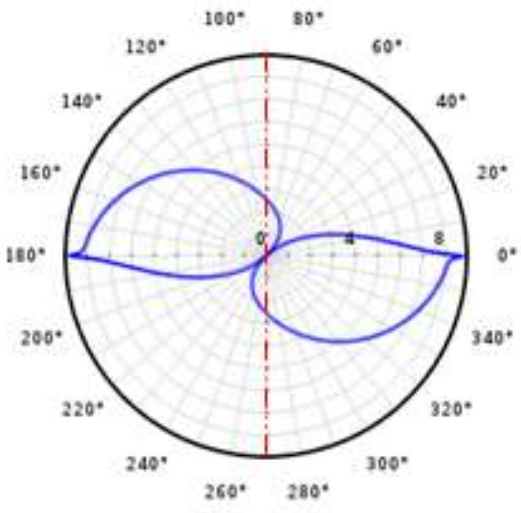


(a)

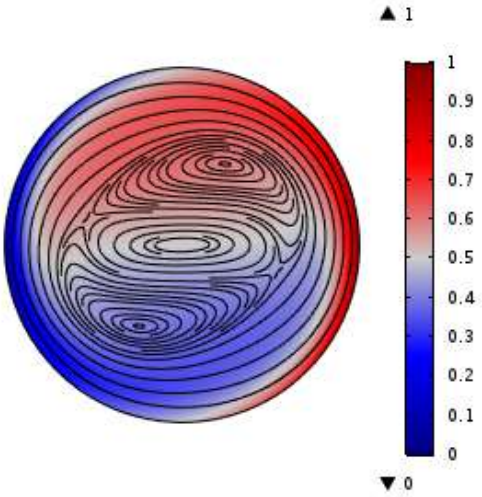


(b)

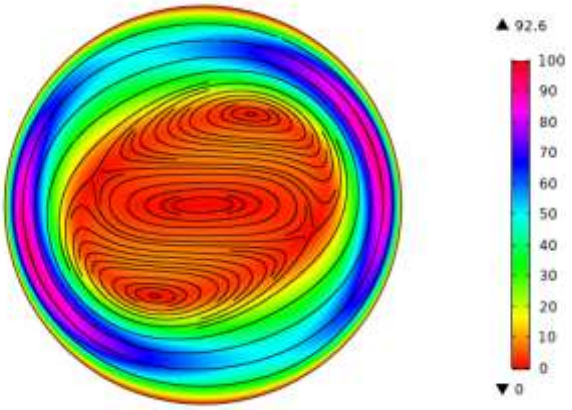


(c)

Fig. 5: Local distributions; Ra = 105, $\phi_0 = 0°$
*(a) Nusselt number; (b) dimensionless velocity; (c) dimensionless temperature*

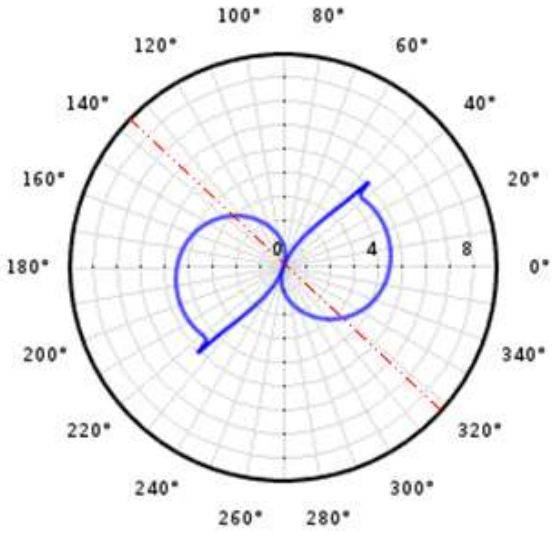


(a)

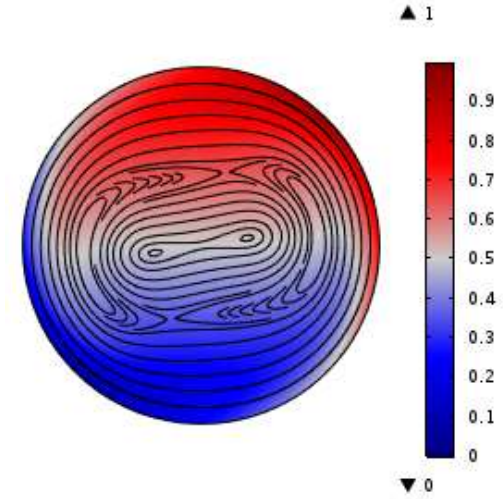


(b)

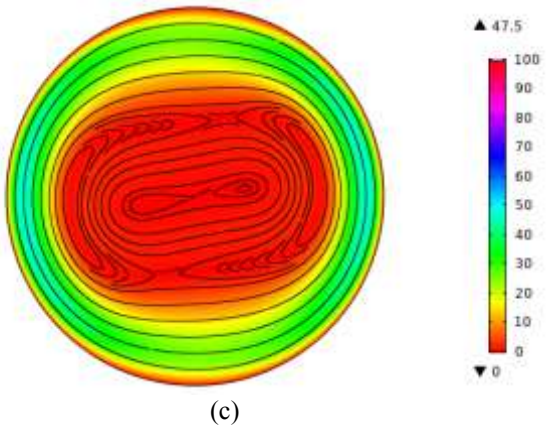


(c)

Fig. 6: Local distributions; Ra = 105, $\phi_0 = +45°$
*(a) Nusselt number; (b) dimensionless velocity; (c) dimensionless temperature*

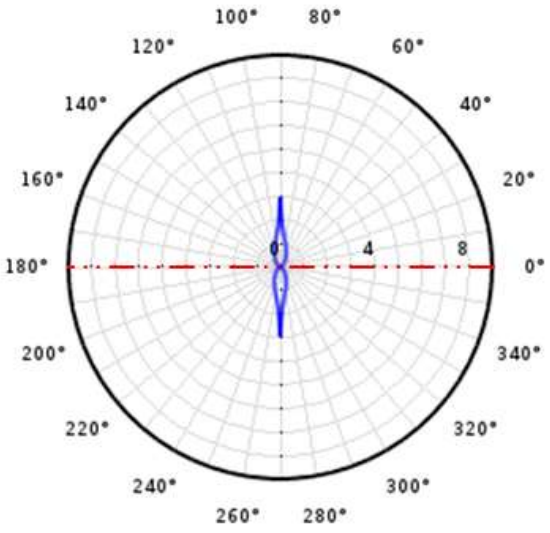


(a)

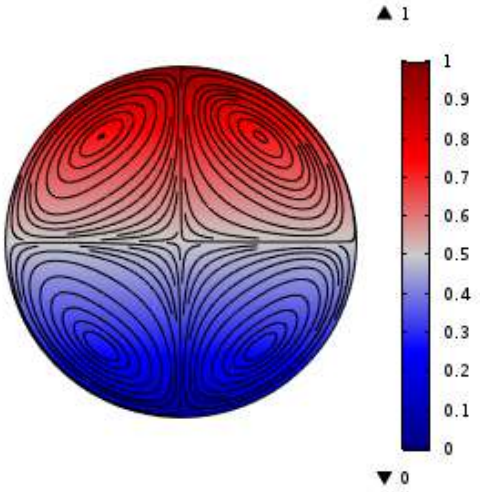


(b)

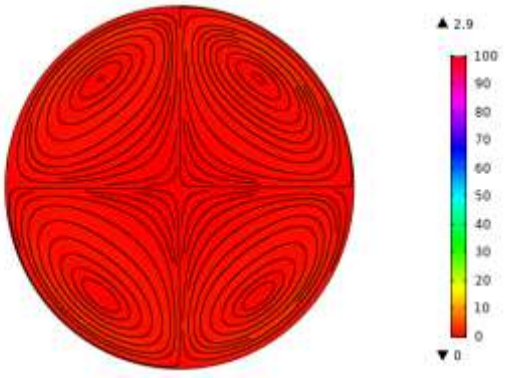


(c)

Fig. 7: Local distributions; Ra = $10^5$, $\phi_0 = +90°$
*(a) Nusselt number; (b) dimensionless velocity; (c) dimensionless temperature*

Figure 7 depicts the local distributions when the heater is centered at 90°. Firstly, it is essential to acknowledge the existence of reduced profiles of the Nusselt number indicating low heat exchanges between the fluid and the wall. Moreover, it is important to point out the appearance of a bi-zone flow with the development of four symmetrical and elliptical counter-rotating convection cells exhibiting eccentric foci and displaying quasi-stratified flow characteristics.

The impact of the heater center and Rayleigh number on average distributions are exposed in Figure 8, Figure 9 and Figure 10. At first blush and according to Figure 8, the heat exchange process is intensified in case the source is centered in the vicinity of 0° and more precisely for high Rayleigh numbers. We also observe a visible change in the flow structure for a heater centered close to -50°. A major transition appears from a single-cell flow to a multicellular flow regime. Note also the visible decreasing profiles of Nusselt numbers for heat sources centered at values greater than 0°. It is also worth mentioning that no significant variations occur in the profile of average Nusselt numbers at low Rayleigh numbers.

Let's not forget to mention that the dimensionless average temperature remains uniform regardless of the heater position and the Rayleigh number at the active wall ($\Theta a = 0.5$).

The profiles of mean dimensionless velocity shown in Figure 9 depict an initial increasing phase for a source centered in [-90°,-70°], attaining an absolute maximum close to -70°. This is accompanied by a subsequent phase between -70° and -40°, indicating a transition in the flow structure from a single-cell flow to a multicellular flow and leading to a strong decrease in average velocity. The final phase between -40° and 90° displays decreasing profiles, which becomes quasi-linear for low Rayleigh numbers. It is interesting to mention the emergence of quasi-stratified flow characteristics in the vicinity of 90°.

Figure 10 depicts the energy efficiency of the heat exchange process based on the Rayleigh number and the center of the heater. One initial point is that for a heater center localized between -90° and 0°, the energy efficiency profiles of the heat exchange process are practically constant. Moreover, very strong increases are observed in the energy efficiency profiles when the heater is centered at [0°,90°]. It should be underlined that in general, the profiles of energy efficiency are more pronounced for low values of the Rayleigh number regardless of the heating position center, except for a source centered in the vicinity of 90°, where the trends are reversed. Given this, the heating process is recommended to be based on temperature step heating along the duct.

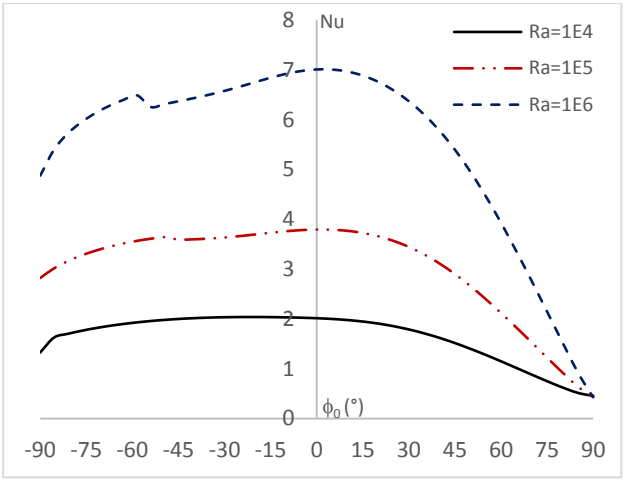


Fig. 8: Average Nusselt number

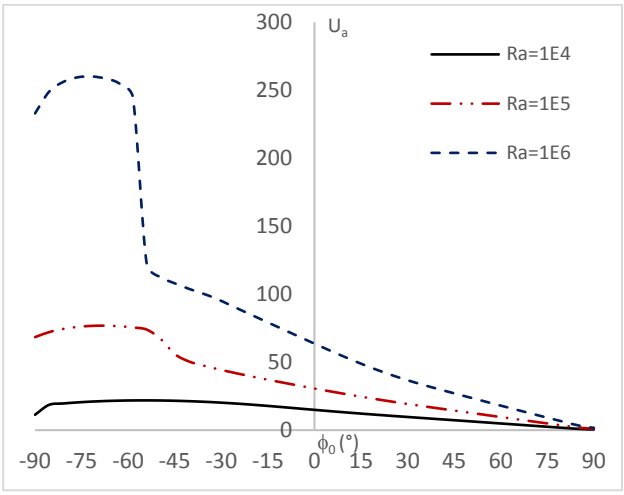


Fig. 9: Average Velocity

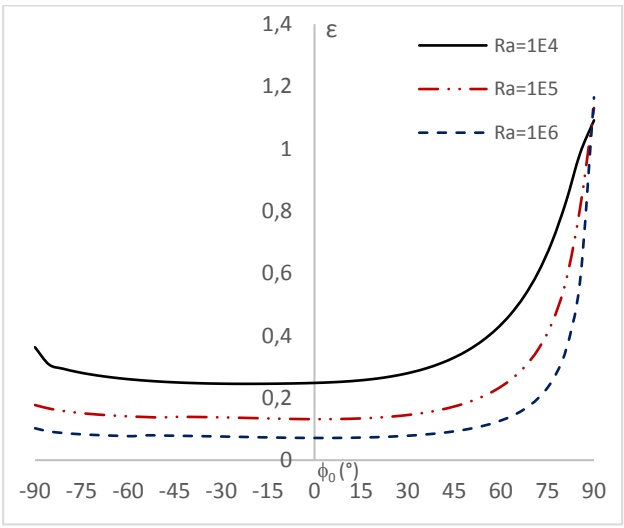


Fig. 10: Energy Efficiency

## 5 Conclusion

The present work describes a numerical investigation of free convection airflow in a horizontal heated cylinder with linear temperature distributions on the walls. The effects of the heater's angular position and the Rayleigh number on fluid flow and heat transfer processes have been numerically examined. Based on the achieved results, it is evident to summarize that the airflow structure is significantly influenced by the heater location. It has been shown that convective heat transfer is enhanced for high Rayleigh numbers and more specifically when the active wall is centered at 0°. It is also worth mentioning that no significant variations occur in the profile of average Nusselt numbers at low Rayleigh numbers. Moreover, the dimensionless average temperature remains consistent irrespective of the Rayleigh number and the placement of the active wall. Furthermore, the optimum energy efficiency level is generally attained for low Rayleigh numbers especially if the heater center is localized at 90°. To conclude, it can be said that the heating process is recommended to be based on temperature step heating along the duct. Subsequent research will focus on assessing thermodynamic irreversibility and entropy generation arising from heat transfer. This aims to enhance both the performance and efficiency of our heating process by employing entropy minimization techniques. One can also consider the numerical modeling of the same problem but in annular configurations.

*References:*

[1] M.B.K. Moortyh, T. Kannan, and K. Senthilvadivu, Effects of radiation on free convection flow past an upward facing horizontal plate in a nanofluid in the presence of internal heat generation. *WSEAS Transactions on Heat and Mass Transfer*, Vol. 10, 2015, pp. 9-20.

[2] A. Mazgar, and F. Ben Nejma, Combined effect of natural convection and non-gray gas radiation with partial heating, *Sādhanā*, Vol.41, No.7, 2016, pp. 805-815.

[3] C. Revnic, and R. Trimbitas, Numerical simulation of MHD natural convection flow in a wavy cavity filled by a hybrid Cu-$Al_2O_3$-water nanofluid with discrete heating, *WSEAS Transactions on Heat and Mass Transfer*, Vol.14, No.9, 2019, pp. 158-166.

[4] T. Djedid, B. Abdelkrim, and Z. Driss, Numerical Study of Heat Transfer by Natural Convection in Concentric Hexagonal Cylinders Charged with a Nanofluid, *WSEAS Transactions on Heat and Mass Transfer*, Vol.17, 2022, pp. 66-79, https://doi.org/10.37394/232012.2022.17.3.

[5] O. Aydin, A. Unal, and T. Ayhan, A numerical study on buoyancy-driven flow in an inclined square enclosure heated and cooled on adjacent walls, *Numerical. Heat Transfer, Part A: Appl*ications, Vol.36, No.6, 1999, pp. 585-599.

[6] M.M. Molla, S.C. Paul, and M.A. Hossain, Natural convection flow from a horizontal circular cylinder with uniform heat flux in presence of heat generation, *Applied Mathematical Modelling*, Vol.33, No.7, 2009, pp. 3226-3236.

[7] M. Corcione, and E. Habib, Buoyant heat transport in fluids across titled square cavities discretely heated at one side, *International Journal of thermal Sciences*, Vol.49, No.5, 2010, pp. 797-808.

[8] P. Loganathan and C. Sivapoornapriya, "Viscous dissipation effects on unsteady natural convective flow past an infinite vertical plate with uniform heat and mass flux," *WSEAS Transactions on Heat and Mass Transfer,* Vol. 9, 2014, pp. 63-73.

[9] K. Jarray, A. Mazgar, and F. Ben Nejma, Effect of combined natural convection and non-gray gas radiation on entropy generation in a circular enclosure with partial heating. *Advances in Mechanical Engineering,* Vol.11, No12, 2019, pp. 1-15.

[10] J. Hernandez, and B. Zamora, Effects of variable properties and non-uniform heating on natural convection flows in vertical channels, *International Journal of Heat and Mass Transfer*, Vol.48, No. 3-4, 2005, pp. 793-807.

[11] E. Natarajan, T. Basak, and S. Roy, Natural convection flows in a trapezoidal enclosure with uniform and non-uniform heating of bottom wall, *International Journal of Heat and Mass Transfer*, Vol.51, No.3-4, 2008, pp. 747-756.

[12] H.F. Oztop, M. Mobedi, E. Abu-Nada, and I. Pop, A heatline analysis of natural convection in a square inclined enclosure filled with a CuO nanofluid under non-uniform wall heating condition, *International Journal of Heat and Mass Transfer,* Vol.55, No.19-20, 2012, pp. 5076-5086.

[13] M. Sathiyamoorthy, and A.J. Chamkha, An Analysis of natural convection in a square cavity with a thin partition for linearly heated side walls, *International Journal of Numerical Methods of Heat and Fluid Flow*, Vol.24, No.5, 2014, pp. 1057-1072.

[14] A. Mohamad, M.A. Sheremet, J. Taler, and P. Ocłoń, Natural convection in differentially heated enclosures subjected to variable temperature boundaries, *International Journal of Numerical Methods of Heat and Fluid Flow*, Vol.29, No.11, 2019, pp. 4130-4141.

[15] B. Şahin, Effects of the center of linear heating position on natural convection and entropy generation in a linearly heated square cavity, *International Communications in Heat and Mass Transfer*, Vol.117, 2020, pp 104675.

[16] T. Yang, B. Wang, J. Wu, Z. Lu, and Q. Zhou, Horizontal convection in a rectangular enclosure driven by a linear temperature profile, *Applied Mathematics and Mechanics*, Vol.42, No.8, 2021, pp. 1183-1190.

[17] M. Turkyilmazoglu, Exponential nonuniform wall heating of a square cavity and natural convection, *Chinese Journal of Physics*, Vol.77, 2022, pp. 2122-2135.

[18] M.S. Astanina, and M.A. Sheremet, Numerical study of natural convection of fluid with temperature-dependent viscosity inside a porous cube under non-uniform heating using local thermal non-equilibrium approach, *International Journal of Thermofluids*, Vol.17, 2023, 100266.

[19] M.M. Taha, I.A. Said, Z. Zeitoun, S. Usman, and M.H. Al-Dahhan, Effect of non-uniform heating on temperature and velocity profiles of buoyancy driven flow in vertical channel of prismatic modular reactor core, *Applied Thermal Engineering*, Vol.225, 2023, 120209.

[20] Z. Liu, D. Yuan, Y. Hao, X. Li, L. Yang, and J. Yao, Experimental study on heat transfer performance of high temperature heat pipe under axial non-uniform heat flux, *Applied Thermal Engineering*, Vol.236, 2024, 121817.

[21] H. Patel, A. Mittal, and T. Nagar, Effect of magnetic field on unsteady mixed convection micropolar nanofluid flow in the presence of non-uniform heat source/sink, *International Journal of Ambient Energy*, Vol.45, 2024, 22667748.

**Contribution of Individual Authors to the Creation of a Scientific Article (Ghostwriting Policy)**

- Akram Mazgar prepared and wrote the manuscript. He also contributed to the numerical simulation of the physical problem on COMSOL software and the verification of the overall research outputs.
- Fayçal Ben Nejma used COMSO MUTILPHYSICS to model the physical problem. He also contributed to the verification of all the results

The authors equally contributed to the present research, at all stages from the formulation of the problem to the final findings and solution.

**Sources of Funding for Research Presented in a Scientific Article or Scientific Article Itself**
No funding was received for conducting this study.

**Conflict of Interest**
The authors have no conflicts of interest to declare.